Published in final edited form as:
Exp Cell Res. 2009 July 15; 315(12): 2001–2011. doi:10.1016/j.yexcr.2009.04.003.

The cytoskeletal scaffold Shank3 is recruited to pathogen-induced actin rearrangements

Alan Huett[*,§], **John M Leong**[†], **Daniel K. Podolsky**[*], and **Ramnik J. Xavier**[*,§]

[*] *Gastrointestinal Unit, Center for the Study of Inflammatory Bowel Diseases, Massachusetts General Hospital, Harvard Medical School, Boston MA, USA*

§ *Center for Computational and Integrative Biology, Massachusetts General Hospital, Harvard Medical School, Boston MA, USA*

† *Department of Molecular Genetics and Microbiology, University of Massachusetts Medical School, Worcester MA, USA*

Summary

The common gastrointestinal pathogens enteropathogenic *Escherichia coli* (EPEC) and *Salmonella* Typhimurium both reorganize the gut epithelial cell actin cytoskeleton to mediate pathogenesis, utilizing mimicry of the host signaling apparatus. The PDZ domain-containing protein Shank3, is a large cytoskeletal scaffold protein with known functions in neuronal morphology and synaptic signaling, and is also capable of acting as a scaffolding adaptor during Ret tyrosine kinase signaling in epithelial cells. Using immunofluorescent and functional RNA-interference approaches we show that Shank3 is present in both EPEC- and *S*. Typhimurium-induced actin rearrangements and is required for optimal EPEC pedestal formation. We propose that Shank3 is one of a number of host synaptic proteins likely to play key roles in bacteria-host interactions.

Keywords

Bacterial infection; attaching and effacing; actin; cytoskeleton; synapse

Introduction

Synapses are specialized multi-protein assemblies which serve to facilitate and organize cellular signals. Many different types of synapses are known, from cell-cell neurological and immune, to virological and bacterially-induced synapses, but most synapses share common features regardless of their origin. Such features include: organization of signaling molecules via scaffolds (often resulting in signal amplification); alterations in membrane shape and trafficking to support optimal signal transfer; and remodeling of the underlying cytoskeletal structure to maximize and maintain synapse contacts. In the case of pathogen-initiated synapses, these host-cell/microbe interactions closely mimic endogenous cell-cell interfaces, either directly co-opting the host signaling machinery or introducing additional microbe-encoded factors to mediate the host-pathogen interface [1–3].

Corresponding author: Ramnik J Xavier, T: 617 643 3331, F: 617 643 3328, Email: E-mail: xavier@molbio.mgh.harvard.edu.

In the immune system synapse formation and subsequent interaction determines how cells regulate both innate and adaptive immunity [4,5], and several PDZ-containing proteins have key roles in these structures [6,7]. PDZ proteins have also been shown to play key roles in the neurological synapse, one such protein is Shank3, which supports the post-synaptic density (PSD) [8,9]. The PSD is a large, complex and ordered array of proteins which serves to mediate neuronal signaling and appears highly conserved over deep evolutionary time. Indeed PSD components, including highly conserved functional interaction domains, can be found in the demosponge *Amphimedon queenslandica*, an organism at the base of the putative animal kingdom, and which lacks neurons and neuronal synapses [10]. This suggests that PSD proteins performed ancient pre-neuronal functions, interacting with their ancient partners in a manner still largely extant, albeit in an altered cellular context. It is therefore plausible that bacteria also exploit these conserved synaptic components, given the long co-evolution of bacteria and animal hosts. In this study we explored the role of the PDZ-containing Shank3 protein in another synaptic signaling context – the interface between bacterial pathogens and human cells, and the subsequent signaling events leading to bacteria-driven actin remodeling.

Studies of Shank proteins have largely concentrated on their roles in the nervous system and PSD, including synaptic potentiation and memory [11]. However, their roles outside of neurons remain largely uncharacterized, despite being expressed in the gut, kidney and other tissues [12]. Shank3 is a scaffold of the PSD and is thought to integrate neurotransmitter receptors and the cortical cytoskeleton. Shank3, and its family members Shank1 and 2, all contain a large number of protein interaction domains, including PDZ, SH3, SAM and proline rich domains. However, for each gene there are multiple alternative spliceforms that lack one or more of these domains. Via their interactions with modulators of small G protein signaling such as cortactin and PIX, they are thought to control actin assembly at the PSD. In addition, neuronal Shank proteins themselves interact with regulators of the actin cytoskeleton: alpha-fodrin, Abp1, IRSp53, and (via IRSp53) the small GTPase Cdc42. Shank2 and 3 and have been shown to recruit Abp1 to dendritic spines and the PSD [8,13,14]. Aside from these cytoskeletal interactions, Shank proteins also interact with the scaffold Homer, serving to regulate calcium stores in response to cell surface glutamate receptors [15–17]. Outside of the nervous system, it is known that Shank3 mediates the signaling from the Ret receptor tyrosine kinase in epithelial cells [18]. Thus Shank3 can be placed between receptor tyrosine kinase activation and downstream actin-dependant and actin-independent signal transduction. Enteropathogenic *Escherichia coli* (EPEC) and other attaching and effacing (A/E) pathogens are major causes of human disease, mainly afflicting children in the developing world, but with a significant emerging foodborne disease component in industrialized nations [19]. All A/E pathogens share a largely conserved pathogenicity island, termed the Locus of Enterocyte Effacement (LEE), which has been horizontally transferred between strains/species [20–22]. The LEE encodes a type III secretion apparatus and associated effectors which serve to attach the bacterium to the host cell via generation of a distinctive A/E lesion, characterized by effacement of microvilli and projection of a pedestal beneath the attached bacterium. This pedestal is composed of actin and associated cytoskeletal components, and its formation is driven by recruitment of host cell signaling molecules to the translocated intimin receptor (Tir). Tir is a bacterial protein inserted into the host cell membrane via the bacterial secretion apparatus [23,24]. Upon binding to intimin on the bacterial surface, the clustering of Tir induces its phosphorylation by host kinases [25–27] and induction of downstream signaling events promoting actin polymerization. This process, clustering, phosphorylation and signaling, strongly resembles endogenous receptor tyrosine phosphorylation signaling [28,29]. It is known that many of the components employed by A/E pathogens for initiation of pedestal signaling play near-identical roles in host signaling pathways [30]. Indeed, it is increasingly clear that the mimicry by pathogens of host signaling pathways and co-option of such signals for infection is common in microbial pathogenesis [1,3].

Other bacterial pathogens, including *Salmonellaenterica* subsp. *enterica* serovar Typhimurium (*S*. Typhimurium), also exploit host actin machinery. In the case of *S*. Typhimurium membrane ruffles are formed which serve to induce bacterial internalization in non-phagocytic cells [31]. While much of the mechanism of this process is known, including the roles of bacterial mimics of G-proteins or G-protein regulators, other aspects still remain undefined, including the roles of focal adhesion proteins recruited to the *Salmonella* entry site [32]. *Salmonella* may induce a focal-adhesion-like structure upon the cell surface, although all the components of this process have yet to be identified.

Shank3 plays a key role in the organization of the massive PSD complex at neuronal synapses, and has been identified as a novel component of receptor tyrosine kinase signaling. Therefore we were interested whether Shank3 might also be involved in other synaptic structures, such as the EPEC pedestal. We reasoned that both host cell receptor tyrosine kinase signaling and EPEC-induced signaling were known to share downstream adaptors, effectors and scaffolds. Thus we embarked upon experiments to determine whether Shank3 is a scaffold involved in the formation of the EPEC pedestal, a well-studied bacterial-host synapse. In addition, with its role in mediating the organization of intercellular contacts such as dendritic spines and synapses, we investigated Shank3 as a candidate for cytoskeletal organization within *Salmonella*-induced invasion ruffles.

Methods

Cell lines and bacterial strains

HeLa cells (line CCL2) were obtained from ATCC. Wild-type and isogenic Nck1 and 2 double knockout mouse embryonic fibroblasts (MEFs) were a kind gift from Dr Tony Pawson. All cell lines were routinely cultured in DMEM supplemented with 10% iron-supplemented calf serum (Hyclone, USA) and 40 μg ml^{-1} gentamycin sulfate. *E. coli* strain E2348/69, used in initial experiments was obtained from Dr Scott Snapper. EPEC strains carrying *tir* deletions and relevant complementation plasmids have been previously described [33]. *S*. Typhimurium SL1344 DsRed2 was given by Dr HC Reinecker.

Transfection of mammalian cells and Shank3 knockdown

HeLa cells were plated onto 18mm glass coverslips in 12 well plates at a density of 1×10^5 cells per well. After 24 hours cells were transfected in antibiotic-free medium with Shank3-HA or HA-vector (a modified pCMV vector, Clontech, USA) using Lipofectamine 2000 (Invitrogen, USA), according to the manufacturer's instructions. Infections were performed after a further 24 hours. MEFs were transfected immediately upon plating, with 1.5×10^5 cells per well and infected 48 hours later.

For shRNA mediated shank3 knockdown we utilized the pSUPER-neoGFP vector (OligoEngine, USA), containing either one of two Shank3-specific RNA targeting sequences (Shank3 shRNA1 or 2) or a non-targeting scrambled sequence (control shRNA). Sense and antisense targeting sequences, separated by a 9-mer hairpin were cloned into the pSUPER-neoGFP vector and sequenced. The RNA-targeting sequences used were: Shank3 shRNA1 – 5′ CCAGCGAUAUCAACCUGAATT 3′; Shank3 shRNA2 – 5′ CAGAGAAGGUCCAAGCUAUTT 3′. Knockdown efficacy was assayed using Shank3 specific real-time quantitive RT-PCR with normalization using GAPDH primers. Shank3 RT-PCR primer sequences were: 5′ GGAGAGCGGGGAACTCACT 3′; 5′ CTGTCCGAGGACTGCTTCAG 3′. Confirmation of knockdown was performed by western blotting of HeLa lysates 48 hours after transfection with control or Shank3-specific shRNA constructs. Lysates were prepared in RIPA buffer and sheared by repeated passage through a 19-gauge needle on ice to release cytoskeletal-associated proteins. Following addition of

loading buffer and boiling, equal volumes were loaded onto two separate gels and blotted for Shank3 (mouse anti-Shank3, Antibodies Incorporated, USA) or β-tubulin (mouse anti-β-tubulin, SantaCruz Biotechnologies, USA). The large size of Shank3 – approximately 200kD – compared to β-tubulin, necessitated the usage of separate SDS-PAGE resolution.

EPEC and *S*. Typhimurium infections

EPEC infections were performed as previously described [34], with slight modifications. Briefly, EPEC colonies were seeded from fresh agar plates into 1.5 ml of LB broth with relevant antibiotics and grown at 37°C with shaking for 9 hours. Cultures were then diluted 1:500 into 5 ml of antibiotic-supplemented DMEM, supplemented with 100mM HEPES (pH7.4). These cultures were grown overnight at 37°C, static in a 5% CO_2 atmosphere. Infections were then performed by diluting overnight cultures 1:1000 into fresh DMEM, supplemented with 20mM HEPES (pH7.4), and adding 1 ml of this mixture into each well of 12-well plates. Following a 10 minute spin at 700×g, plates were incubated at 37°C, 5% CO_2 for 4–6 hours.

S. Typhimurium infections were performed as previously described [35]. Briefly, SL1344 colonies from fresh agar plates were grown in LB plus 100 μg ml^{-1} ampicillin, shaking at 37° C overnight. Cultures were diluted 1:33 in fresh LB plus ampicillin and grown for a further 3 hours. Infections were performed using 1:100 dilutions of these sub-cultures, yielding an multiplicity of infection of 1:100. For the purposes of examining bacterial-induced ruffles infections were allowed to proceed for 20 minutes.

Immunostaining

Following infection, transfected cells were washed twice in PBS and fixed in 4% formaldehyde solution in PBS for 20 minutes. Cells were then permeabilised in 0.1% Triton-X100 in PBS for 2 minutes, blocked with 2% BSA for 40 minutes and stained using appropriate antibodies for one hour. For staining of endogenous Shank3 we utilized a methanol fixation procedure, cells were fixed in ice-cold 100% methanol for 2 minutes, washed twice in PBS, extracted with 0.1% Triton X100 in PBS for 5 minutes and blocked for 10 minutes in 1% BSA. Primary antibodies against Shank3 and actin were then applied for one hour, followed by extensive washing. Primary antibodies used were: mouse anti-HA (Covance, USA); mouse anti-Shank3 (Antibodies Incorporated, USA) and rabbit anti-actin (Sigma Aldrich, USA). Secondary antibodies were obtained from Molecular Probes (Invitrogen USA) and were highly cross-adsorbed: Alexa488-conjugated goat anti-mouse, Alexa488-conjugated goat anti rabbit and Alexa568-conjugated goat anti rabbit. Actin was stained in formalin-fixed samples using Alexa633-conjugated phalloidin (Invitrogen) and DNA staining for bacterial localization used either propidium iodide or DAPI (Invitrogen). Following staining and washing, coverslips were mounted in a glycerol-base medium (PolySciences, USA) and imaged on either a BioRad Radiance 2000 or Leica SP5 confocal microscopes. Image analysis and export was performed with the appropriate manufacturer's software. For pedestal cross-sections RGB images were imported as stacks into ImageJ [36] and intensity data through selected pedestals collected using the "plot profile" function.

Assessment of EPEC attachment and pedestal formation

Following infection and staining of either HeLa or MEF cells lines as described, we selected transfected cells by either Shank3 expression (via anti-HA staining) or, in the case of shRNA experiments, GFP expression. Total numbers of bacteria attached to cells were counted by DAPI staining and the numbers of EPEC exhibiting phalloidin-dense F-actin staining beneath them were recorded. Overall percentages of pedestal-attached bacteria were calculated based upon at least 40 cells per condition; significance was assessed using a two-sample T-test and 95% confidence intervals calculated.

To quantify the proportion of pedestals exhibiting Shank3-HA recruitment an operator blinded to the experimental condition identified attached bacteria via DAPI staining, the number of these bacteria exhibiting actin foci and HA-staining were recorded and the data subsequently analysed. At least 40 cells per condition were counted.

Results

Shank3, but not Shank1, is recruited to EPEC-induced pedestals

HeLa cells were transfected with plasmids encoding either Shank3-HA or empty vector (containing the HA epitope tag) and infected with EPEC 24 hours later. Following three to five hours of infection, cells were washed, fixed and stained for immunofluorescence. We observed that Shank3-HA was found in EPEC pedestals, colocalizing with actin throughout the length of the pedestal (Figure 1A). As a control for antibody cross-reaction, vector alone (Figure 1B) and overexpressed Shank1-HA, a protein closely-related to Shank3 (Figure 1C), showed no such pedestal staining using identical antibodies and incubation conditions. We confirmed these observations by plotting staining intensity profiles across representative pedestals, examples are shown in Figure 1D. We were able to clearly see that actin and Shank3-HA colocalized, whereas Shank1-HA or HA vector alone did not yield actin-colocalized staining. We did not observe any increase in either EPEC attachment or pedestal formation (as assessed by F-actin staining) in HeLa cells transfected with Shank1-HA or Shank3-HA (Table 1). Counting of pedestals and HA-staining beneath attached bacteria confirmed that pedestal-located HA-staining was confined to cells expressing Shank3-HA and largely absent from those expressing Shank1-HA (Table 1).

Shank3 is recruited to the EPEC pedestal in an Nck-independent manner

EPEC-induced pedestal formation closely resembles endogenous receptor tyrosine kinase signaling. The secreted bacterial protein Tir is embedded within the host cell membrane following secretion into the host cell. Upon ligation to the bacterial membrane protein intimin, Tir clusters beneath the bacterial cell. Tyrosine phosphorylation of Y474 in the Tir C-terminus is mediated by host kinases, in a manner akin to host receptor phosphorylation [26,27]. Once phosphorylated, Tir clusters are able to recruit the host cytoskeletal adaptor protein, Nck, via an interaction between the Nck SH2 domain and a Tir motif mimicking the endogenous Nck-binding domain of nephrin [30,37]. Binding of Nck results in recruitment and activation of the Arp2/3 complex and subsequent actin polymerization, with Tir/Nck acting as the initiating nucleus. This Nck-dependant pedestal formation pathway dominates in classical wild-type EPEC strains, however there are also two, less efficient Nck-independent pathways [38,39]. One of these pathways requires Y474, while the other requires Tir residue Y454, and for neither are the factors that result in initiation of actin nucleation conclusively identified (see Discussion). It is plausible that the presence of parallel pathways reflects differential optimization of actin polymerization during initial pedestal formation and subsequent pedestal maintenance. To further examine the role of Shank3 in the EPEC pedestal we utilized Nck1 and 2 double knockout MEFs and isogenic control MEFs, as previously described [38,40]. These cells were transfected with Shank3-HA or HA-vector and subsequently infected with EPEC for five to seven hours prior to fixation and staining. Knockout MEFs were able to support pedestal formation, albeit at a much lower rate than control cells; 9% (+/− 1.8) of attached bacteria formed pedestals in $Nck^{-/-}$ MEFs, compared to 77% (+/− 2.4) in Nck replete cells, similar to previous reports [38]. Confocal microscopy revealed that Shank3-HA was located to pedestals regardless of the presence or absence of Nck (Figure 2A). Similar results were obtained with endogenous staining for Shank3 – staining was observed in pedestals in both control and Nck knockout cells (Figure 2B). These colocalisations were confirmed through intensity cross-sections of selected pedestals, representative profiles are shown in Figure 2C). In the absence of Nck, we observed Shank3 within a subset of pedestals. However,

Nck-independent pedestals are both shorter and less frequent than those formed on Nck-replete MEFs [34], and we suggest the slower kinetics and lower efficiency of Nck-independent pedestal growth may result in some pedestals that have not recruited sufficient Shank3 for immunodetection. Also, in $Nck^{-/-}$ cells we did observe Shank3 enrichment at a small proportion (10%, +/− 2.8) of sites of bacterial attachment in the absence of visible actin rearrangement. However, similar Shank3 staining was not observed in cells where Nck was available. This was suggestive of Shank3 recruitment prior to (or at the very early stages of) actin pedestal formation, revealed by the poorer recruitment of actin in the absence of Nck. Therefore, we set out to further dissect the requirements for Shank3 recruitment.

Shank3 localisation to the sites of bacterial attachment is Tir-dependant

Since we had observed Shank3 staining in EPEC pedestals occurred independent of Nck, we tested the requirement for Tir in Shank3 recruitment. EPEC lacking Tir was unable to recruit actin to sites of bacterial attachment, whereas the same strain complemented with wild-type Tir generated robust actin pedestals (Table 2). Similarly, Shank3 recruitment to bacterial attachment sites was absent in Tir-deficient infections, but was maintained in the control infections. Therefore we concluded that Shank3 recruitment was dependant upon Tir.

Using bacterial strains expressing solely Tir molecules lacking one or both of the key tyrosine phosphorylation sites, we observed that Y454 was not required for Shank3 recruitment, with rates of bacteria-Shank3 colocalisation approaching wild-type (Table 2). Levels of actin pedestal formation were very low during infections of Tir Y474F and Tir Y454F/Y474F-expressing bacteria, however we did not observe any Shank3-localisation around adherent, but non-pedestal-forming ΔTir, Y474F- or Y454F/Y474F-expressing bacteria. This was in contrast to the small proportion of such events observed in $Nck^{-/-}$ cells when infecting with wild-type EPEC. These data suggested that the actin-independent localization of Shank3 seen in Nck-deficient cells was not due to attachment-mediated Shank3 recruitment, but likely reflected poor staining of actin caused by the reduced actin polymerisation previously observed in these cells during EPEC infection.

Shank3 is also recruited to Salmonella-induced actin rearrangements

Following our identification of Shank3 as a molecule recruited to EPEC pedestals we investigated whether it was involved in another pathogen-induced actin rearrangement, the internalization of *S*. Typhimurium. Overexpression of HA-tagged Shank3 during *S*. Typhimurium infection of HeLa cells showed a clear colocalization of Shank3-HA to actin-rich membrane ruffles, both ruffles and strong Shank3/actin association were absent in uninfected cells (Figure 3A). Staining of endogenous Shank3 during *S*. Typhimurium infection also revealed a significant enrichment within *Salmonella*-induced ruffles. Ruffles were clearly stained with anti-Shank3 antibodies, and Shank3 largely co-located with actin (Figure 3B, HeLa cells) in these structures. Absence of Nck had no effect upon *S*. Typhimurium-induced ruffles, and actin ruffles induced by *S*. Typhimurium on Nck-deficient cells were also associated with Shank3 (Figure 3B, WT and Nck−/−). Thus we had identified two pathogen-induced actin rearrangements that were associated with Shank3. Shank3 had been identified as having important functions in receptor tyrosine kinase and calcium/Homer signaling. We were interested whether Shank3 localization at actin pedestals and/or actin ruffles was purely as a structural/scaffold component, or whether Shank3 might also play an active role in mediating signaling during host-pathogen interactions. Therefore, we set out to investigate the roles of Shank3 in EPEC actin pedestal formation using a functional RNAi approach.

Ablation of Shank3 using RNAi results in a modest reduction in pedestal formation efficiency

We transfected HeLa cells and MEFs with shRNAs directed against Shank3, or a scrambled non-targeting sequence, and determined effective RNA knockdown by quantitative RT-PCR.

Shank3-targetting vectors significantly reduced Shank3 mRNA and protein levels (Figure 4A) in transfected HeLa cells after 48 hours. Due to relatively low transfection efficiency in MEF cells lines, we utilized the GFP reporter co-expressed with the shRNA hairpin to select transfected cells for counting, thus ensuring that consistently transfected population were assayed. Thus it is likely that in both HeLa cells and MEFs the population sampled for pedestal quantitation exhibited higher levels of Shank3 knockdown than RT-PCR or Western analysis of the pooled HeLa population would suggest.

Infection of Shank3-knockdown cells with EPEC resulted in a modest, but reproducible and significant reduction in the number of actin pedestals formed beneath attached bacteria in HeLa cells and both Nck-replete and knockout MEFs when compared to appropriate control-shRNA transfected cells (Figure 4B). A similar modest reduction in pedestal formation was observed after knock down of Shank3 on Nck-deficient MEFs, but this difference failed to reach statistical significance, likely due to the very low rate of attachment in $Nck^{-/-}$ MEFs. Rates of bacterial attachment were unaffected by Shank3 knockdown, suggesting that Shank3 plays a role solely in pedestal growth and not initial attachment. We did not observe any increase in the rate of pedestal formation in MEFs overexpressing Shank3-HA, either in the presence, or absence of Nck (data not shown). Likewise, we were unable to observe any consistent qualitative differences in pedestal intensity, shape or length in the absence of Shank3 compared to controls.

Discussion

Shank3 is a cytoskeletal scaffold protein recruited to both the EPEC pedestal and *S*. Typhimurium-induced membrane ruffles

Despite their diverse locations and components, synapses share common functional features and optimizations to fulfill their functions as signaling foci. Whilst some synaptic structures are relatively short-lived (e.g. the T/B cell immunological synapse), others are capable of persistent, albeit dynamic, stability – such as neuronal synapses. Such large, long-lived synapses are maintained by an array of cytoskeletal and cellular junctional rearrangements, as well as constant signals derived from the synaptic interface itself. In the case of EPEC, the creation of a stable synapse enables adherence and colonization of the gastro-intestinal tract. For *S*. Typhimurium, the interaction at the cell membrane is short-lived, but is followed by internalization and exploitation of host cytosolic traffic from within the *Salmonella*-containing vacuole [41].

Shank3 has been mostly studied for its role within the post-synaptic density, where it is though to act as a “master scaffold” and mediate overall organization and architecture of the PSD. However, it has also been implicated as a scaffolding adaptor for the Ret tyrosine kinase – and therefore may play a role in both epithelial turnover and mucosal immune development [42]. In this paper we demonstrate for the first time that the Shank3 scaffold protein is located within both actin-rich pedestals induced by the A/E pathogen EPEC and Salmonella-induced membrane ruffles. The formation of A/E pedestals shares many of the features of endogenous tyrosine kinase signaling, including crucial phosphorylation sites and recruitment of host adaptors and downstream signal generation. Therefore it is likely that these pathogens utilize host scaffold molecules as a result of their subversion of upstream factors.

Shank3 recruitment was dependant on Tir, and bacterial adherence to cells alone was insufficient to trigger Shank3-bacteria colocalisation. Tir residue Y474, which is critical for Tir recognition by Nck, was required for recruitment, but Shank3 localized to pedestals independent of Nck. Two other host factors that both bind Tir and localize to actin pedestals have been shown to interact with Shank3, and thus could promote Shank3 recruitment. First, IRSp53 [43] and its homolog IRTKS bind EHEC Tir and are present in both EPEC and EHEC

pedestals [44,45]. However, IRSp53 and IRTKS recognize an EHEC Tir sequence containing the homolog of EPEC Tir Y454, suggesting that these factors are not responsible for Shank3 recruitment, which depends on Y474. Secondly, cortactin, a cytoskeletal protein targeted by EPEC, EHEC and other bacterial pathogens, is found throughout the actin pedestal [46–48].

Recruitment of Shank3 was generally associated with detectable actin pedestals. In Nck-deficient cells, we observed a small proportion of adherent bacteria that appeared to recruit Shank3 in the absence of actin rearrangement, but the (antibody-mediated) actin staining method required to visualize pedestals in those cells was significantly less sensitive than the (phalloidin-mediated) staining utilized with other cells. We therefore believe that the apparently actin-independent Shank3 recruitment observed in Nck-deficient MEFs may be due to poor detection of the shorter, weaker Nck-independent pedestals, and not a truly actin-independent phenomenon.

Thus, we find it likely that Shank3 is recruited subsequent to pedestal initiation, possibly as a molecule that organizes and maintains pedestal integrity as it extends and persists. shRNA knockdown of Shank3 modestly reduced the efficiency of pedestal generation, and pedestal formation was not significantly increased by overexpression of Shank3. The lack of dramatic effect on pedestal formation, however, could be due to redundant function of other scaffolds in the EPEC pedestal. Indeed there are two other known Shank proteins in humans, although Shank1 did not locate to the pedestal these studies, Shank2 also contains many similar domains to Shank3. There are also multiple differentially spliced isoforms of all the known Shank family members, and therefore it is possible that our shRNA knockdown was not effective against all Shank3 isoforms. Junctional proteins, such as IQGAP, are translocated to the EPEC pedestal and these may play a role in maintenance of the long-lived, dynamic pedestal interface between the colonizing pathogen and host cell [49]. This finding is consistent with the hypothesis that scaffold usage by EPEC is diverse, akin to the broad array of kinase, adaptors and actin polymerization pathways used by EPEC, EHEC and related bacteria [25,34,38,39,50,51].

It has also been demonstrated that Shank3 was also recruited to *S*. Typhimurium-induced membrane ruffles, structures induced via GTPase activation, molecular mimicry and actin nucleation and stabilization. These structures are quite different from the EPEC pedestal and thus Shank3 may be a widely used molecule in a variety of cytoskeletal contexts. It is of interest that *S*. Typhimurium is thought to recruit focal adhesion proteins to the apical cell surface during invasion. Although the exact roles for focal adhesion proteins here are not known they appear to serve an organizational role essential for bacterial entry [32]. The PSD is a large and highly organized structure, with Shank3 thought to be present as the central scaffold. It is possible that other cellular cytoskeletal (re)organizations also rely upon Shank3 as a master scaffold and regulator of signaling. In this paper we identify Shank3 as a component of both the actin-rich pedestal and ruffles induced by EPEC and *S*. Typhimurium, respectively, on both human and mouse cells. We suggest that Shank3 acts as one of a number of cytoskeletal components which mediate the growth and stability of large actin-driven membrane structures. Shank3 has an established role in the signal transduction of Ret receptor tyrosine kinase, and our finding that it is also involved in the EPEC pedestal highlights the similarities between endogenous host and pathogen-driven signaling pathways. It also illustrates the power of bacterial mimicry of host processes to subvert the cytoskeleton, without entirely perturbing cellular architecture, or inducing innate defense responses. We propose that Shank3 may play many roles within epithelial cells related to actin cytoskeleton organization. As shown by recruitment to Salmonella-induced ruffles and its ability to elevate EPEC-induced pedestal attachment, as a master scaffold Shank3 is capable of mediating both structural organization and signaling. Here we also present an example of such cytoskeletal organization, where Shank3 is used by EPEC to assist in the creation of a stable interface between host cells and the bacterial pathogen.

Acknowledgments

We would like to thank Tony Pawson (Mount Sinai Hospital, Toronto Canada) for his kind gift of Nck 1 and 2 double knockout and isogenic wild-type MEFs. *Salmonella* Typhimurium Sl1344 DsRed2 was a gift from Dr HC Reinecker (Massachusetts General Hospital, Boston), and EPEC E2348/69 was obtained from Dr S Snapper (Massachusetts General Hospital). This work was supported by grants from the National Institutes of Health to RJX (NIH AI062773), JML (AI46454) and DKP (DK060049 and DK043351).

References

1. Alto NM, Shao F, Lazar CS, Brost RL, Chua G, Mattoo S, McMahon SA, Ghosh P, Hughes TR, Boone C, Dixon JE. Identification of a bacterial type III effector family with G protein mimicry functions. Cell 2006;124:133–145. [PubMed: 16413487]
2. Arbeloa A, Bulgin RR, MacKenzie G, Shaw RK, Pallen MJ, Crepin VF, Berger CN, Frankel G. Subversion of actin dynamics by EspM effectors of attaching and effacing bacterial pathogens. Cellular microbiology 2008;10:1429–1441. [PubMed: 18331467]
3. Sallee NA, Rivera GM, Dueber JE, Vasilescu D, Mullins RD, Mayer BJ, Lim WA. The pathogen protein EspF(U) hijacks actin polymerization using mimicry and multivalency. Nature. 2008
4. Gonzalez PA, Prado CE, Leiva ED, Carreno LJ, Bueno SM, Riedel CA, Kalergis AM. Respiratory syncytial virus impairs T cell activation by preventing synapse assembly with dendritic cells. Proceedings of the National Academy of Sciences of the United States of America 2008;105:14999–15004. [PubMed: 18818306]
5. Bloom O, Unternaehrer JJ, Jiang A, Shin JS, Delamarre L, Allen P, Mellman I. Spinophilin participates in information transfer at immunological synapses. The Journal of cell biology 2008;181:203–211. [PubMed: 18411312]
6. Xavier R, Rabizadeh S, Ishiguro K, Andre N, Ortiz JB, Wachtel H, Morris DG, Lopez-Ilasaca M, Shaw AC, Swat W, Seed B. Discs large (Dlg1) complexes in lymphocyte activation. The Journal of cell biology 2004;166:173–178. [PubMed: 15263016]
7. Ludford-Menting MJ, Oliaro J, Sacirbegovic F, Cheah ET, Pedersen N, Thomas SJ, Pasam A, Iazzolino R, Dow LE, Waterhouse NJ, Murphy A, Ellis S, Smyth MJ, Kershaw MH, Darcy PK, Humbert PO, Russell SM. A network of PDZ-containing proteins regulates T cell polarity and morphology during migration and immunological synapse formation. Immunity 2005;22:737–748. [PubMed: 15963788]
8. Qualmann B, Boeckers TM, Jeromin M, Gundelfinger ED, Kessels MM. Linkage of the actin cytoskeleton to the postsynaptic density via direct interactions of Abp1 with the ProSAP/Shank family. J Neurosci 2004;24:2481–2495. [PubMed: 15014124]
9. Baron MK, Boeckers TM, Vaida B, Faham S, Gingery M, Sawaya MR, Salyer D, Gundelfinger ED, Bowie JU. An architectural framework that may lie at the core of the postsynaptic density. Science (New York, NY 2006;311:531–535.
10. Sakarya O, Armstrong KA, Adamska M, Adamski M, Wang IF, Tidor B, Degnan BM, Oakley TH, Kosik KS. A post-synaptic scaffold at the origin of the animal kingdom. PLoS ONE 2007;2:e506. [PubMed: 17551586]
11. Hung AY, Futai K, Sala C, Valtschanoff JG, Ryu J, Woodworth MA, Kidd FL, Sung CC, Miyakawa T, Bear MF, Weinberg RJ, Sheng M. Smaller dendritic spines, weaker synaptic transmission, but enhanced spatial learning in mice lacking Shank1. J Neurosci 2008;28:1697–1708. [PubMed: 18272690]
12. Berglund L, Bjorling E, Oksvold P, Fagerberg L, Asplund A, Szigyarto CA, Persson A, Ottosson J, Wernerus H, Nilsson P, Lundberg E, Sivertsson A, Navani S, Wester K, Kampf C, Hober S, Ponten F, Uhlen M. A genecentric human protein atlas for expression profiles based on antibodies. Mol Cell Proteomics 2008;7:2019–2027. [PubMed: 18669619]
13. Bockers TM, Mameza MG, Kreutz MR, Bockmann J, Weise C, Buck F, Richter D, Gundelfinger ED, Kreienkamp HJ. Synaptic scaffolding proteins in rat brain. Ankyrin repeats of the multidomain Shank protein family interact with the cytoskeletal protein alpha-fodrin. The Journal of biological chemistry 2001;276:40104–40112. [PubMed: 11509555]

14. Soltau M, Richter D, Kreienkamp HJ. The insulin receptor substrate IRSp53 links postsynaptic shank1 to the small G-protein cdc42. Molecular and cellular neurosciences 2002;21:575–583. [PubMed: 12504591]
15. Sala C, Roussignol G, Meldolesi J, Fagni L. Key role of the postsynaptic density scaffold proteins Shank and Homer in the functional architecture of Ca2+ homeostasis at dendritic spines in hippocampal neurons. J Neurosci 2005;25:4587–4592. [PubMed: 15872106]
16. Xiao B, Tu JC, Worley PF. Homer: a link between neural activity and glutamate receptor function. Current opinion in neurobiology 2000;10:370–374. [PubMed: 10851183]
17. Tu JC, Xiao B, Naisbitt S, Yuan JP, Petralia RS, Brakeman P, Doan A, Aakalu VK, Lanahan AA, Sheng M, Worley PF. Coupling of mGluR/Homer and PSD-95 complexes by the Shank family of postsynaptic density proteins. Neuron 1999;23:583–592. [PubMed: 10433269]
18. Schuetz G, Rosario M, Grimm J, Boeckers TM, Gundelfinger ED, Birchmeier W. The neuronal scaffold protein Shank3 mediates signaling and biological function of the receptor tyrosine kinase Ret in epithelial cells. The Journal of cell biology 2004;167:945–952. [PubMed: 15569713]
19. Kaper JB, Nataro JP, Mobley HL. Pathogenic Escherichia coli. Nature reviews 2004;2:123–140.
20. Abe H, Miyahara A, Oshima T, Tashiro K, Ogura Y, Kuhara S, Ogasawara N, Hayashi T, Tobe T. Global Regulation by Horizontally Transferred Regulators Establishes the Pathogenicity of Escherichia coli. DNA Res 2008;15:25–38. [PubMed: 18222925]
21. Deng W, Li Y, Vallance BA, Finlay BB. Locus of enterocyte effacement from Citrobacter rodentium: sequence analysis and evidence for horizontal transfer among attaching and effacing pathogens. Infection and immunity 2001;69:6323–6335. [PubMed: 11553577]
22. Muniesa M, Schembri MA, Hauf N, Chakraborty T. Active genetic elements present in the locus of enterocyte effacement in Escherichia coli O26 and their role in mobility. Infection and immunity 2006;74:4190–4199. [PubMed: 16790794]
23. Kenny B, DeVinney R, Stein M, Reinscheid DJ, Frey EA, Finlay BB. Enteropathogenic E. coli (EPEC) transfers its receptor for intimate adherence into mammalian cells. Cell 1997;91:511–520. [PubMed: 9390560]
24. Ebel F, Podzadel T, Rohde M, Kresse AU, Kramer S, Deibel C, Guzman CA, Chakraborty T. Initial binding of Shiga toxin-producing Escherichia coli to host cells and subsequent induction of actin rearrangements depend on filamentous EspA-containing surface appendages. Molecular microbiology 1998;30:147–161. [PubMed: 9786192]
25. Bommarius B, Maxwell D, Swimm A, Leung S, Corbett A, Bornmann W, Kalman D. Enteropathogenic Escherichia coli Tir is an SH2/3 ligand that recruits and activates tyrosine kinases required for pedestal formation. Molecular microbiology 2007;63:1748–1768. [PubMed: 17367393]
26. Phillips N, Hayward RD, Koronakis V. Phosphorylation of the enteropathogenic E. coli receptor by the Src-family kinase c-Fyn triggers actin pedestal formation. Nature cell biology 2004;6:618–625.
27. Swimm A, Bommarius B, Li Y, Cheng D, Reeves P, Sherman M, Veach D, Bornmann W, Kalman D. Enteropathogenic Escherichia coli use redundant tyrosine kinases to form actin pedestals. Molecular biology of the cell 2004;15:3520–3529. [PubMed: 15155808]
28. Frankel G, Phillips AD. Attaching effacing Escherichia coli and paradigms of Tir-triggered actin polymerization: getting off the pedestal. Cellular microbiology 2008;10:549–556. [PubMed: 18053003]
29. Hayward RD, Leong JM, Koronakis V, Campellone KG. Exploiting pathogenic Escherichia coli to model transmembrane receptor signalling. Nature reviews 2006;4:358–370.
30. Blasutig IM, New LA, Thanabalasuriar A, Dayarathna TK, Goudreault M, Quaggin SE, Li SS, Gruenheid S, Jones N, Pawson T. Phosphorylated YDXV motifs and Nck SH2/SH3 adaptors act cooperatively to induce actin reorganization. Molecular and cellular biology 2008;28:2035–2046. [PubMed: 18212058]
31. Schlumberger MC, Hardt WD. Salmonella type III secretion effectors: pulling the host cell's strings. Current opinion in microbiology 2006;9:46–54. [PubMed: 16406778]
32. Shi J, Casanova JE. Invasion of host cells by Salmonella typhimurium requires focal adhesion kinase and p130Cas. Molecular biology of the cell 2006;17:4698–4708. [PubMed: 16914515]

33. Campellone KG, Giese A, Tipper DJ, Leong JM. A tyrosine-phosphorylated 12-amino-acid sequence of enteropathogenic Escherichia coli Tir binds the host adaptor protein Nck and is required for Nck localization to actin pedestals. Molecular microbiology 2002;43:1227–1241. [PubMed: 11918809]
34. Campellone KG, Robbins D, Leong JM. EspFU is a translocated EHEC effector that interacts with Tir and N-WASP and promotes Nck-independent actin assembly. Developmental cell 2004;7:217–228. [PubMed: 15296718]
35. Rioux JD, Xavier RJ, Taylor KD, Silverberg MS, Goyette P, Huett A, Green T, Kuballa P, Barmada MM, Datta LW, Shugart YY, Griffiths AM, Targan SR, Ippoliti AF, Bernard EJ, Mei L, Nicolae DL, Regueiro M, Schumm LP, Steinhart AH, Rotter JI, Duerr RH, Cho JH, Daly MJ, Brant SR. Genome-wide association study identifies new susceptibility loci for Crohn disease and implicates autophagy in disease pathogenesis. Nature genetics 2007;39:596–604. [PubMed: 17435756]
36. Collins TJ. ImageJ for microscopy. BioTechniques 2007;43:25–30. [PubMed: 17936939]
37. Jones N, Blasutig IM, Eremina V, Ruston JM, Bladt F, Li H, Huang H, Larose L, Li SS, Takano T, Quaggin SE, Pawson T. Nck adaptor proteins link nephrin to the actin cytoskeleton of kidney podocytes. Nature 2006;440:818–823. [PubMed: 16525419]
38. Campellone KG, Leong JM. Nck-independent actin assembly is mediated by two phosphorylated tyrosines within enteropathogenic Escherichia coli Tir. Molecular microbiology 2005;56:416–432. [PubMed: 15813734]
39. Brady MJ, Campellone KG, Ghildiyal M, Leong JM. Enterohaemorrhagic and enteropathogenic Escherichia coli Tir proteins trigger a common Nck-independent actin assembly pathway. Cellular microbiology 2007;9:2242–2253. [PubMed: 17521329]
40. Bladt F, Aippersbach E, Gelkop S, Strasser GA, Nash P, Tafuri A, Gertler FB, Pawson T. The murine Nck SH2/SH3 adaptors are important for the development of mesoderm-derived embryonic structures and for regulating the cellular actin network. Molecular and cellular biology 2003;23:4586–4597. [PubMed: 12808099]
41. Bakowski M, Braun V, Brumell JH. Salmonella-containing vacuoles: directing traffic and nesting to grow. Traffic (Copenhagen, Denmark). 2008
42. Veiga-Fernandes H, Coles MC, Foster KE, Patel A, Williams A, Natarajan D, Barlow A, Pachnis V, Kioussis D. Tyrosine kinase receptor RET is a key regulator of Peyer's patch organogenesis. Nature 2007;446:547–551. [PubMed: 17322904]
43. Bockmann J, Kreutz MR, Gundelfinger ED, Bockers TM. ProSAP/Shank postsynaptic density proteins interact with insulin receptor tyrosine kinase substrate IRSp53. Journal of neurochemistry 2002;83:1013–1017. [PubMed: 12421375]
44. Vingadassalom D, Kazlauskas A, Skehan BM, Cheng HC, Magoun L, Robbins D, Rosen MK, Saksela K, Leong JM. Insulin Receptor Tyrosine Kinase Substrate links the E. coli O157:H7 actin assembly effectors Tir and EspFU during pedestal formation. PNAS In Press. 2009
45. Weiss SM, Ladwein M, Schmidt D, Ehinger J, Lommel S, Jänsch L, Gunzer F, Rottner K, Stradal TEB. IRSp53 links the enterohemorrhagic E. coli effectors Tir and EspFU for actin pedestal formation. Cell Host and Microbe In Press. 2009
46. Cantarelli VV, Takahashi A, Akeda Y, Nagayama K, Honda T. Interaction of enteropathogenic or enterohemorrhagic Escherichia coli with HeLa cells results in translocation of cortactin to the bacterial adherence site. Infection and immunity 2000;68:382–386. [PubMed: 10603412]
47. Cantarelli VV, Takahashi A, Yanagihara I, Akeda Y, Imura K, Kodama T, Kono G, Sato Y, Iida T, Honda T. Cortactin is necessary for F-actin accumulation in pedestal structures induced by enteropathogenic Escherichia coli infection. Infection and immunity 2002;70:2206–2209. [PubMed: 11895988]
48. Cantarelli VV, Kodama T, Nijstad N, Abolghait SK, Nada S, Okada M, Iida T, Honda T. Tyrosine phosphorylation controls cortactin binding to two enterohaemorrhagic Escherichia coli effectors: Tir and EspFu/TccP. Cellular microbiology 2007;9:1782–1795. [PubMed: 17451412]
49. Peralta-Ramirez J, Hernandez JM, Manning-Cela R, Luna-Munoz J, Garcia-Tovar C, Nougayrede JP, Oswald E, Navarro-Garcia F. EspF Interacts with nucleation-promoting factors to recruit junctional proteins into pedestals for pedestal maturation and disruption of paracellular permeability. Infection and immunity 2008;76:3854–3868. [PubMed: 18559425]

50. Garmendia J, Phillips AD, Carlier MF, Chong Y, Schuller S, Marches O, Dahan S, Oswald E, Shaw RK, Knutton S, Frankel G. TccP is an enterohaemorrhagic Escherichia coli O157:H7 type III effector protein that couples Tir to the actin-cytoskeleton. Cellular microbiology 2004;6:1167–1183. [PubMed: 15527496]

51. Patel A, Cummings N, Batchelor M, Hill PJ, Dubois T, Mellits KH, Frankel G, Connerton I. Host protein interactions with enteropathogenic Escherichia coli (EPEC): 14-3-3tau binds Tir and has a role in EPEC-induced actin polymerization. Cellular microbiology 2006;8:55–71. [PubMed: 16367866]

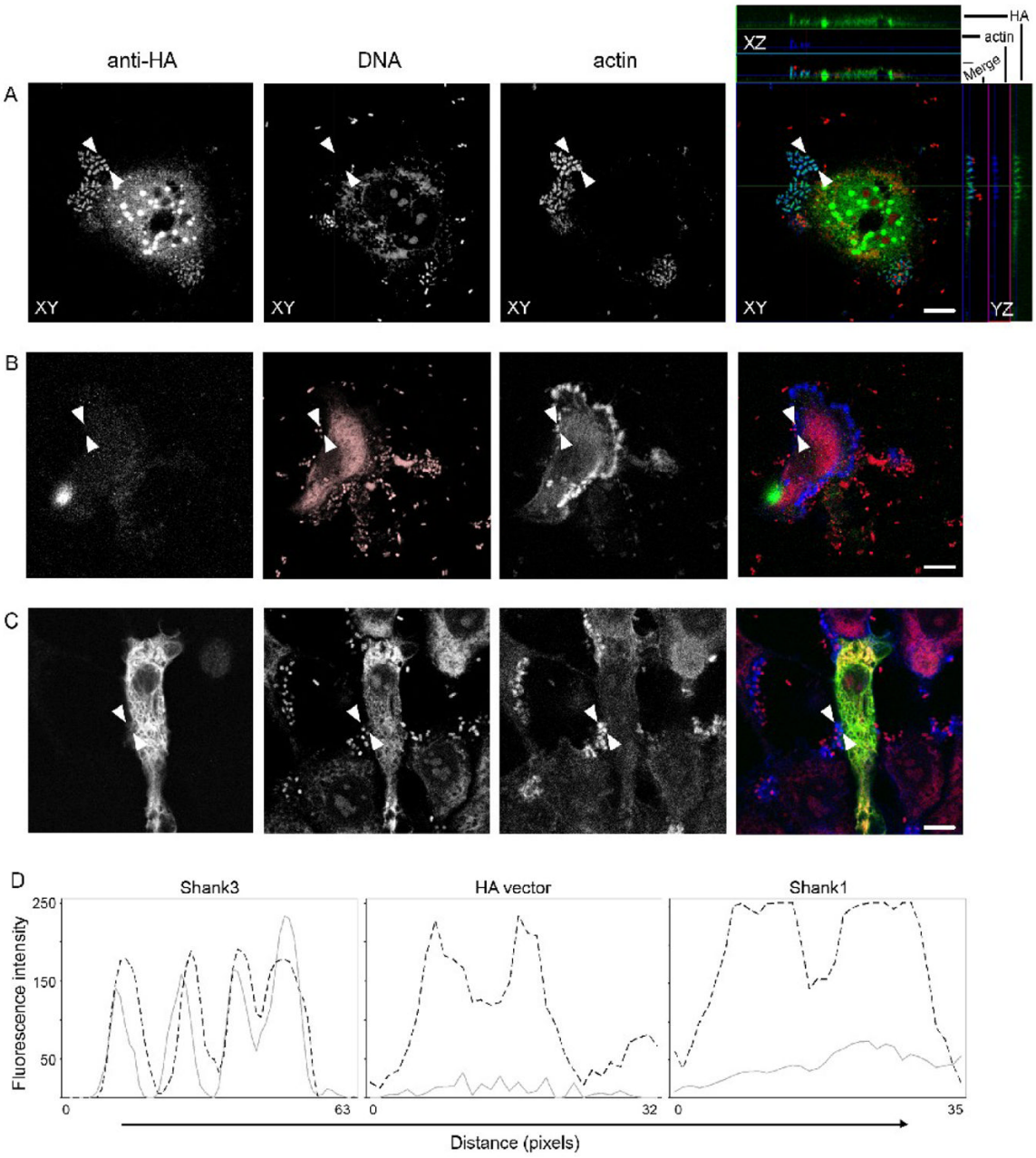

Figure 1. Shank3 is recruited to the EPEC pedestal

HeLa cells were transfected with either Shank3-HA (A), HA vector alone (B) or Shank1-HA (C). After 24 hours cells were infected with EPEC for four hours, washed, fixed and stained using anti-HA antibodies, propidium iodide and phalloidin. Anti-HA (green in merge), DNA (red in merge) and actin (blue in merge) are shown, as single plane maximum projections, with orthogonal projections in the case of Shank3-HA, of confocal z-stacks. Scale bars represent 10 μm. (D) Fluorescent intensity profiles of actin (dotted line) and anti-HA (grey line) staining are shown. Pedestal profiles were drawn as straight lines between the arrowheads shown in the micrographs. In contrast to the colocalisation seen with Shank3 (A), HA or Shank1 (B and C) staining are both largely absent staining beneath attached bacteria.

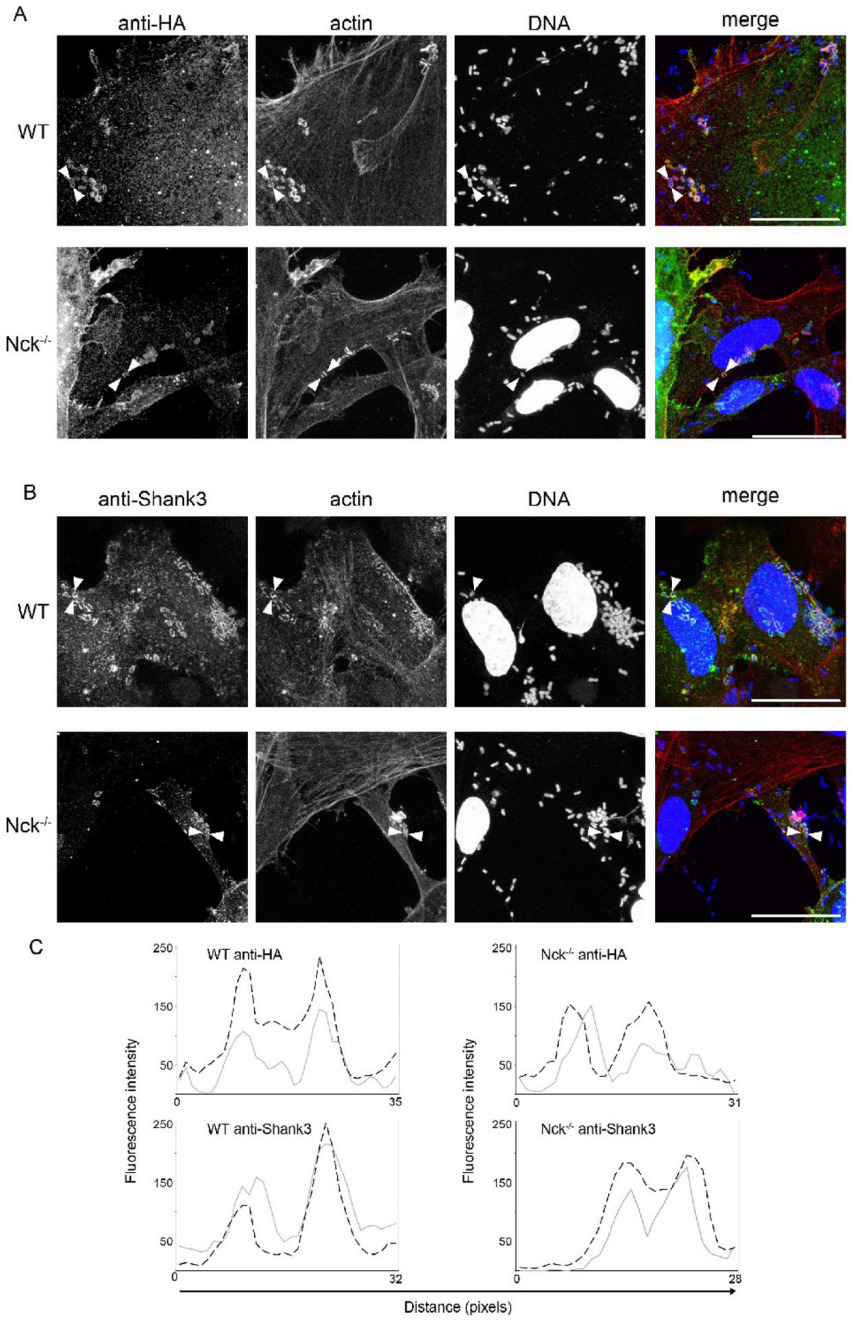

Figure 2. Shank3 localization to pedestals is independent of Nck

(A) Isogenic mouse embryonic fibroblasts expressing both Nck1 and 2 (WT), or lacking Nck1 and 2 expression ($Nck^{-/-}$) were transfected with Shank3-HA and infected with EPEC for six hours as described. Cells were then fixed and stained using anti-HA antibodies. (B) Untransfected MEFs were infected with EPEC for six hours and stained for endogenous Shank3 with specific antibodies. Following washing and staining, cells were examined by confocal microscopy. Single plane maximum projections of infected cells stained with anti-HA or shank3 antibodies (green in merge), DAPI (blue in merge) and phalloidin (red in merge) are shown. Scale bars represent 10 μm. (C) Fluorescent intensity profiles of actin (dotted line) and anti-HA (grey line) staining are shown. Pedestal profiles were drawn as straight lines between

the arrowheads shown in the micrographs. Note the clear actin co-localisation present in both HA-tagged and endogenous Shank3 staining.

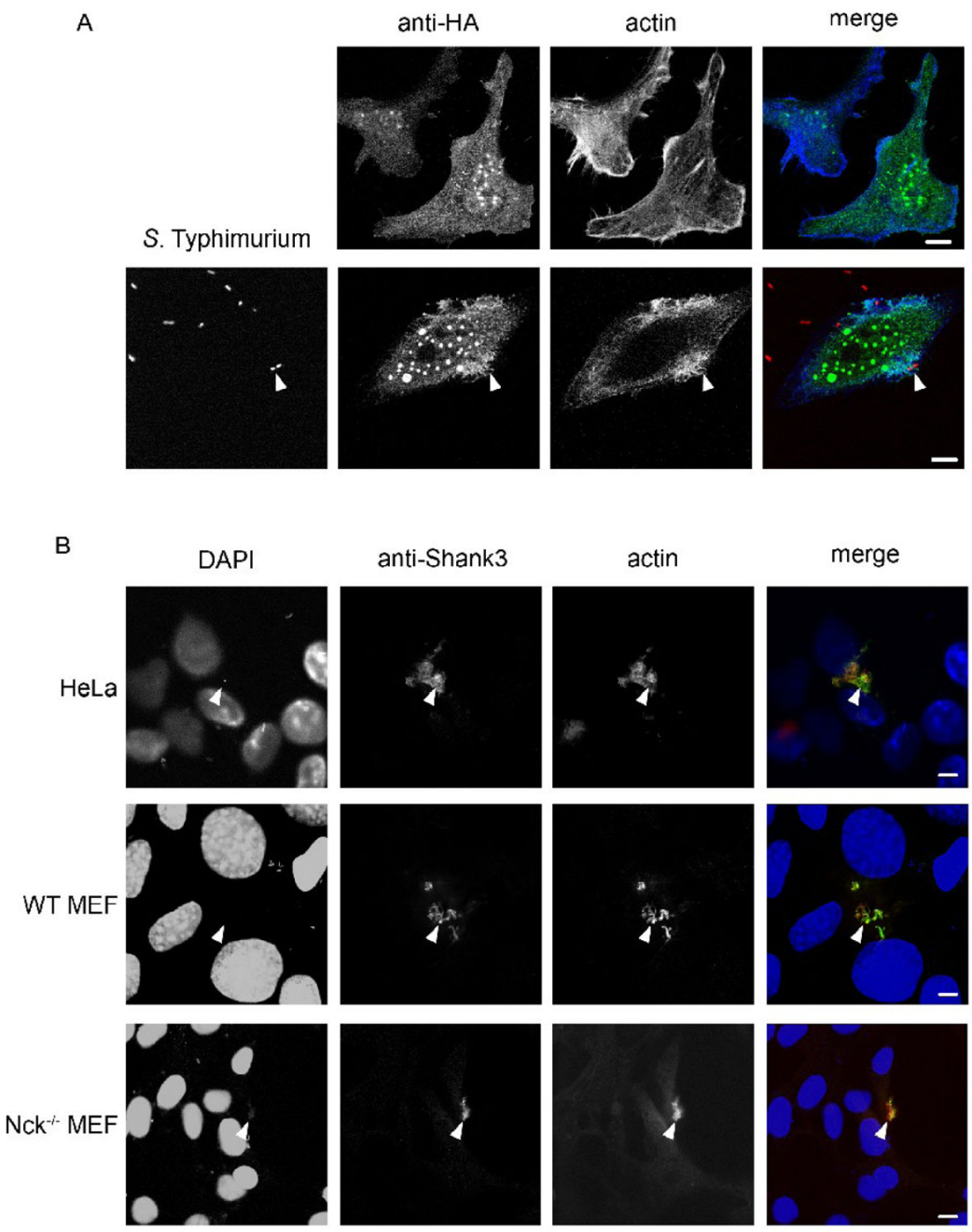

Figure 3. Shank3 is recruited to Salmonella-induced membrane ruffles

(A) HeLa cells were transfected with Shank3-HA and stained with anti-HA antibodies (top panels). Identically transfected cells were infected with *S*. Typhimurium and fixed and stained 20 minutes following bacterial exposure to capture invasion events (bottom panels). Anti-HA (green in merge), actin (blue in merge) and bacteria (red in merge) are shown as maximum confocal projections. Arrows indicate sites of bacteria-induced ruffling. Scale bars represent 10 μm.

(B) HeLa, WT or $Nck^{-/-}$ MEFs were infected for 20 minutes with *S*. Typhimurium and stained with DAPI (blue in merge), anti-Shank3 (green in merge) and anti-actin (red in merge)

antibodies. Arrows mark pronounced dorsal actin- and Shank3-rich ruffles. Images shown are single confocal optical sections. Scale bars represent 10 μm.

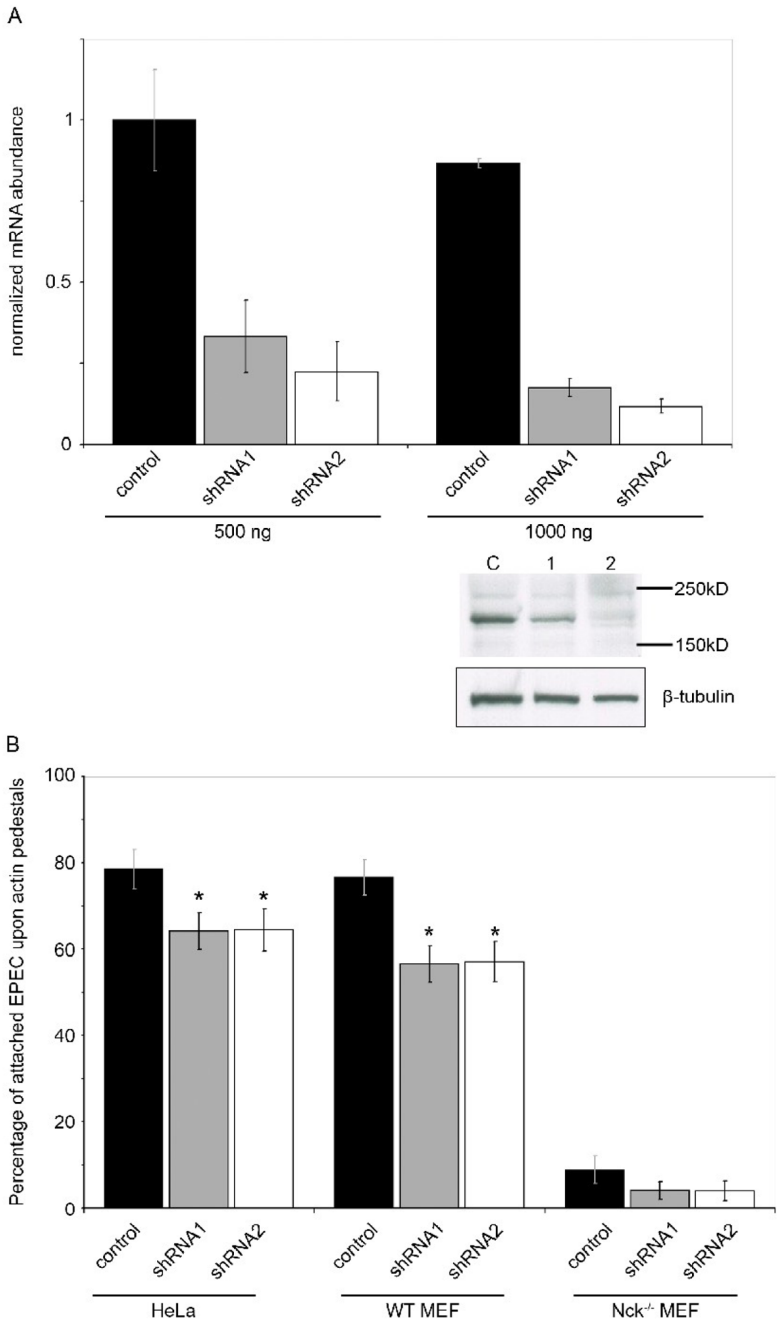

Figure 4. Shank3 deficient cells are less able to support efficient EPEC pedestal formation

(A) HeLa cells were transfected with two levels of control shRNA vector (black bars) or one of two shank3-targeting shRNA vectors (grey and white bars). After 48 hours knockdown was assessed using real-time quantitative RT-PCR with Shank3 specific primers and normalized to GAPDH. Shown are means of two experiments, each using two independent cDNA samples, with standard deviations. A representative western blot following high-level (1000 ng) transfection of shRNA vectors is shown. Levels of endogenous Shank3 (as determined with anti-Shank3 antibody) are reduced in cells receiving Shank3-directed shRNAs 1 and 2, compared to control-transfected cells. Anti-tubulin is shown as a protein-level control.

(B) HeLa cells, WT MEFs or Nck−/− MEFs were transfected with shRNA constructs for 48 hours, then infected with EPEC for 6 hours as described. Pedestal formation was assessed by F-actin staining and is expressed as a percentage of total adherent bacteria. Means of data pooled from three independent experiments are shown, at least 40 cells per condition were counted in each experiment. Error bars indicate 95% confidence intervals, * signifies statistical significance $p<0.05$. Significance was measured using a two-sample T-test, comparing to the relevant shRNA control samples. Data is representative of three independent experiments.

Table 1

Shank3, but not Shank1 is recruited to actin pedestals in EPEC-infected HeLa cells.

	Bacteria/cell	Pedestals/100 bacteria	HA-staining/100 bacteria
HA vector	8.2 (+/− 1.8)	82.3 (+/− 2.8)	1.2 (+/− 2.2)
Shank1-HA	7.6 (+/− 1.5)	80.2 (+/− 3.1)	4.9 (+/− 1.6)
Shank3-HA	7.8 (+/− 1.6)	79.3 (+/− 4.2)	63.3 (+/− 2.8)

HeLa cells were infected with wild-type EPEC for 3 hours, 24h after transfection with either HA vector or Shank-HA constructs. Bacterial attachment, pedestal formation and HA-staining were quantified in two separate experiments by an operator blinded to the experimental condition. Figures represent means and standard deviations from data pooled from two experiments.

Table 2

Shank3 recruitment to EPEC attachment is Tir-dependant

	Bacteria/cell	Pedestals/100 bacteria	Shank3-staining/100 bacteria
ΔTir	3.2 (+/− 1.1)	0.0 (+/− 0.0)	0.2 (+/− 0.3)
pTir	7.3 (+/− 0.9)	73.1 (+/− 3.1)	41.3 (+/− 2.2)
Y454F	8.2 (+/− 1.4)	68.2 (+/− 2.3)	35.1 (+/− 3.1)
Y474F	2.2 (+/− 1.2)	4.1 (+/− 3.2)	0.2 (+/− 0.5)
Y454F/Y474F	1.8 (+/− 1.3)	0.3 (+/− 0.4)	0.1 (+/− 0.2)

HeLa cells were transfected with Shank3-HA and infected 24 hours later. Infections were performed using EPEC expressing wild-type or mutant Tir variants for 5 hours, cells were then fixed and stained for bacteria, actin and Shank3. Shank3 staining was performed using anti-Shank3 antibodies since bacterial Tir expression constructs were HA-fusions. Quantification was performed by a blinded operator and data was pooled from two independent experiments and is presented as means with standard deviations.